Eur. Phys. J. D **9**, 575–579 (1999)

THE EUROPEAN PHYSICAL JOURNAL D

EDP Sciences

Monodispersive Cr cluster formation by plasma-gas-condensation method

S. Yamamuro[a,b], K. Sumiyama, M. Sakurai, and K. Suzuki

Institute for Materials Research, Tohoku University, Sendai 980-8577, Japan

Received: 31 August 1998 / Received in final form: 5 November 1998

Abstract. Nanometer–sized Cr clusters in the size rage of 8.5–13 nm have been produced by a plasma gas condensation-type cluster deposition apparatus, which combines a glow–discharge sputtering technique with an inert gas condensation technique. We have studied the effects of sputter power, Ar gas pressure, P_{Ar}, and Ar gas flow rate, V_{Ar}, on the size distribution of Cr clusters by transmission electron microscopy. The cluster size is insensitive to the sputter power, while the nucleation process is promoted when the sputter power is increased. Monodispersive Cr clusters are formed at both low P_{Ar} and low V_{Ar}, where the nucleation and growth processes are definitely separated, and the coagulation of growing particles is prohibited. In the present experiments, these conditions are effectively attained by the use of a carrier gas flow and liquid nitrogen cooling of the cluster growth region.

PACS. 36.40.-c Atomic and molecular clusters – 61.46.+w Clusters, nanoparticles, and nanocrystalline materials – 81.10.Bk Growth from vapor

1 Introduction

Cluster assembling is a new material fabrication process for obtaining nanoscale-controlled functional materials using nanometric clusters as building blocks [1]. For this purpose, it is crucial to produce monodispersive clusters, because the properties of cluster-assembled materials strongly depend on the cluster size. Recently, we have constructed an intensive and size-controllable cluster deposition system, i.e., a plasma-gas-condensation (PGC)-type cluster deposition apparatus [2–4] which is similar to the one originally developed by Haberland *et al.* [5]. The PGC method combines a grow–discharge sputtering technique with an inert gas condensation technique: metal vapor is generated by sputtering at about 150 Pa pressure and condenses into clusters in a carrier gas flow. In contrast to conventional thermal evaporation sources, this method is advantageous for generating clusters consisting of refractive or low vapor-pressure metals because any kind of metal can be vaporized by sputtering. In the present report, we demonstrate monodispersive Cr cluster formation using the PGC method, and elucidate its process by studying through transmission electron microscopy (TEM) how process parameters (the Ar gas pressure, Ar gas flow rate, and sputter power) influence the formed clusters.

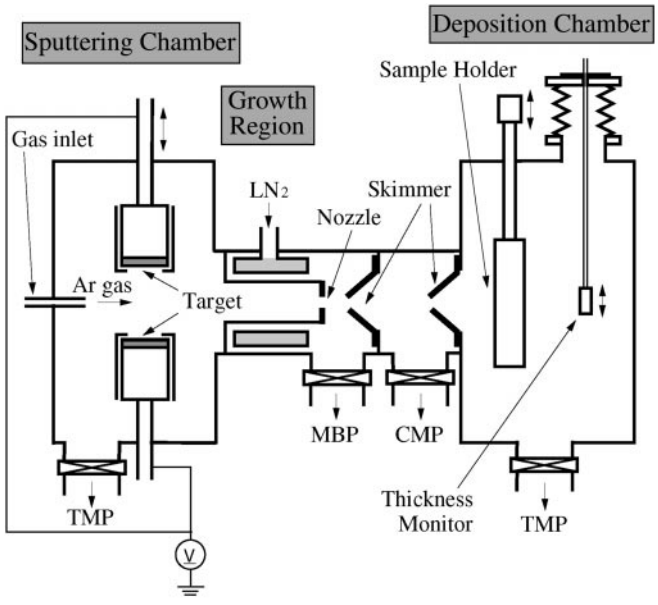

Fig. 1. Schematic drawing of the plasma-gas-condensation (PGC)-type cluster deposition apparatus. TMP, MBP, and CMP represent the turbo-molecular pump, mechanical booster pump, and combination molecular pump, respectively.

2 Experiment

Figure 1 shows a schematic drawing of the PGC apparatus. It mainly consists of three components: a sputtering chamber, a liquid-nitrogen-cooled growth region, and

[a] Core Research for Evolutional Science and Technology (CREST) of Japan Science and Technology (JST) Corporation, 4-1-8 Honchou, Kawaguchi, Saitama 332-0012, Japan

[b] e-mail: yamamuro@snap8.imr.tohoku.ac.jp

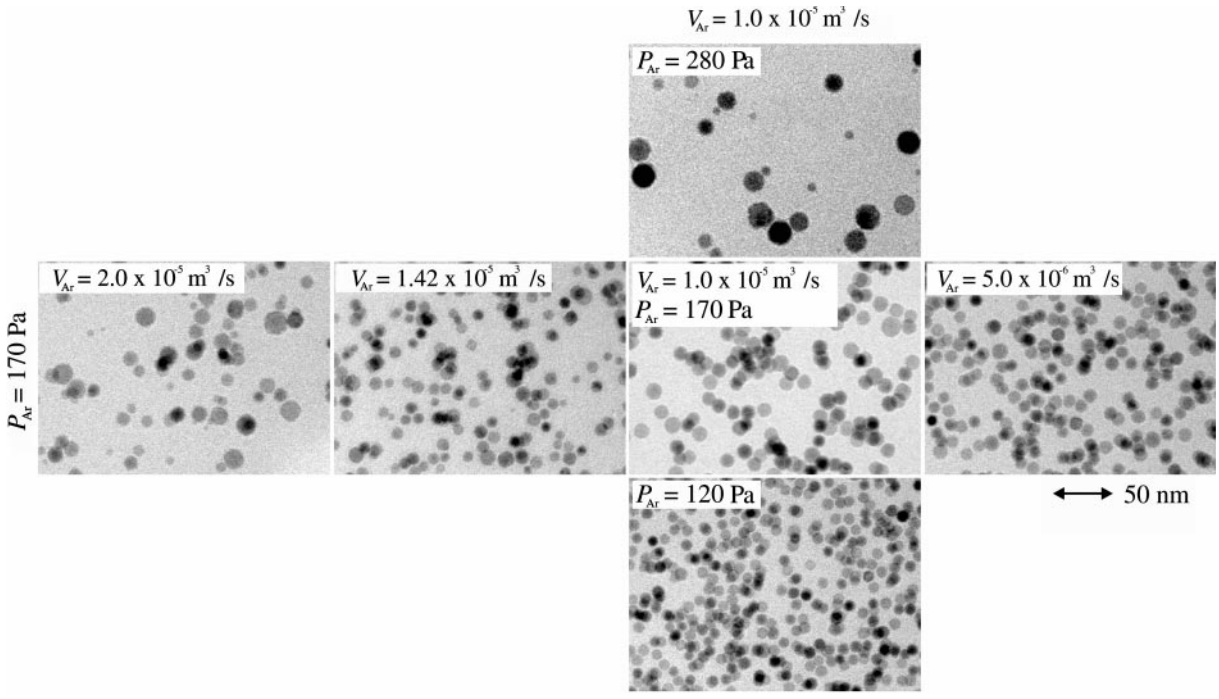

Fig. 2. Bright-field TEM images of Cr clusters produced by variation of the Ar gas pressure, P_{Ar}, and the Ar gas flow rate, V_{Ar}, independently: $P_{\mathrm{Ar}} = 120\,\mathrm{Pa} - 280\,\mathrm{Pa}$ at a constant $V_{\mathrm{Ar}} = 1.0 \times 10^{-5}\,\mathrm{m}^3/\mathrm{s}$, and $V_{\mathrm{Ar}} = 5.0 \times 10^{-6}$–$2.0 \times 10^{-5}\,\mathrm{m}^3/\mathrm{s}$ at a constant $P_{\mathrm{Ar}} = 170\,\mathrm{Pa}$.

a deposition chamber. A facing target-type DC sputtering source, which combines a hollow-cathode discharge mode and a magnetron mode, was operated at a high Ar gas pressure, P_{Ar}, of 120–280 Pa to vaporize Cr targets of 70 mm in diameter. The distance between the two targets was 100 mm. The magnetic field of about 20 mT was applied to the space between the two targets to get a high ionization rate of Ar gas and a high sputtering rate. A large amount of Ar gas (the Ar gas flow rate $V_{\mathrm{Ar}} = 5.0 \times 10^{-6}$–$2.0 \times 10^{-5}\,\mathrm{m}^3/\mathrm{s}$ at 273 K and 1.0×10^5 Pa) was injected continuously into the sputtering chamber from a gas inlet, and effectively evacuated by a mechanical booster pump (MBP) through a small nozzle, whose typical diameter was 3.5 mm. Clusters were formed in a carrier gas flow, ejected through the small nozzle and two skimmers by differential pumping, and then deposited onto a TEM microgrid fixed on a sample holder in the deposition chamber ($\sim 1 \times 10^{-2}$ Pa). The substrate temperature was at about 300 K during the deposition. If the nozzle diameter is varied adequately, P_{Ar} and V_{Ar} can be controlled independently. The input power for sputtering was 300 W, except for the experiments in power dependence of the cluster size distribution. The Cr clusters were deposited in the deposition chamber with the effective thickness of 2 nm, which was measured by a quartz oscillator-type thickness monitor. The deposition rate was 2×10^{-3}–7×10^{-2} nm/s, depending on the experimental conditions. To clarify the cluster formation region, we deposited clusters for five minutes at three positions: the sputtering chamber, and the entrance and the exit of the growth region. We observed cluster images using a 200-kV Hitachi HF-2000 TEM, and estimated their size distribution using image-analysis software.

3 Results

Figure 2 shows the TEM images of Cr clusters deposited with varying V_{Ar} and P_{Ar} independently. The uniformly sized Cr clusters are observed for $P_{\mathrm{Ar}} \leq 170$ Pa and $V_{\mathrm{Ar}} \leq 1.0 \times 10^{-5}\,\mathrm{m}^3/\mathrm{s}$, whereas the size distribution becomes markedly broad at $P_{\mathrm{Ar}} = 280$ Pa and $V_{\mathrm{Ar}} = 2 \times 10^{-5}\,\mathrm{m}^3/\mathrm{s}$. The mean cluster diameter and standard deviation estimated from these images are shown in Fig. 3. The standard deviations (the mean cluster diameters) of such uniformly sized clusters are 0.5 nm (10.4 nm), 0.7 nm (8.6 nm), and 1.1 nm (11.7 nm) at $P_{\mathrm{Ar}} = 170$ Pa ($V_{\mathrm{Ar}} = 5.0 \times 10^{-6}\,\mathrm{m}^3/\mathrm{s}$), 120 Pa ($1.0 \times 10^{-5}\,\mathrm{m}^3/\mathrm{s}$), and 170 Pa ($1.0 \times 10^{-5}\,\mathrm{m}^3/\mathrm{s}$), respectively. These values of the standard deviation are less than 10% of the mean cluster diameter, showing a good monodispersivity.

As shown in Fig. 4, the deposition rate of clusters rapidly increases when the sputter power is increased above 100 W; however, it becomes negligible below 100 W. As shown in the inset of Fig. 4, the cluster size is insensitive to the input power in this power region. These results indicate that the nucleation is promoted with an increase in the input power.

In order to understand the cluster formation process, we captured growing Cr clusters in the sputtering chamber and the growth region also, and then observed them by TEM (see Fig. 5). For $P_{\mathrm{Ar}} = 170$ Pa

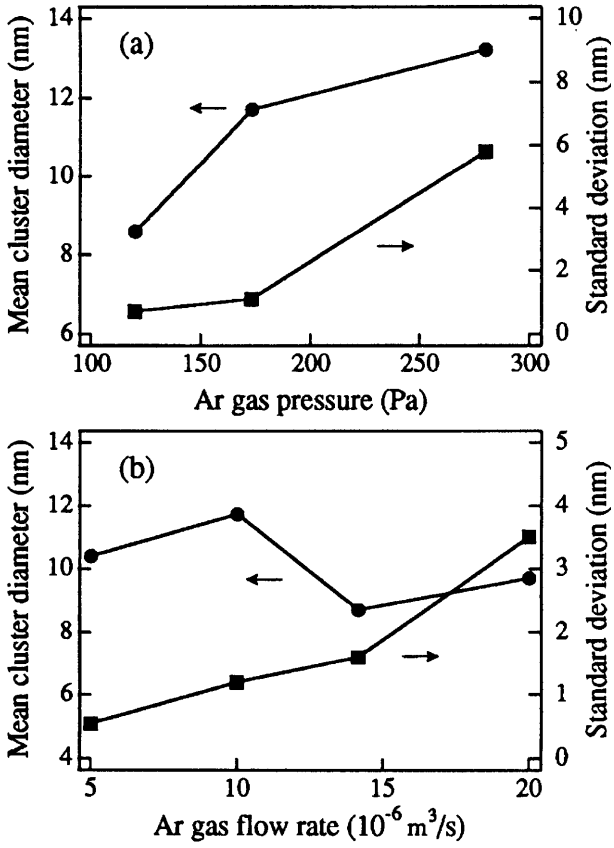

Fig. 3. Mean cluster diameter and standard deviation as a function of (a) the Ar gas pressure, P_{Ar}, and (b) the Ar gas flow rate, V_{Ar}, estimated from Fig. 2.

($V_{\mathrm{Ar}} = 5.0 \times 10^{-6}\,\mathrm{m}^3/\mathrm{s}$), there exists only island morphology without any clusters at the positions of either the sputtering target or the entrance to the growth region. However, small clusters are observed at the exit from the growth region, indicating that the clusters nucleate and grow only in the liquid nitrogen-cooled growth region. For $P_{\mathrm{Ar}} = 280\,\mathrm{Pa}$ ($V_{\mathrm{Ar}} = 1.0 \times 10^{-5}\,\mathrm{m}^3/\mathrm{s}$), large clusters (some of them exceeding 100 nm in diameter) are formed even near the sputtering targets and at the entrance to the growth region. However, such large clusters suddenly disappear at the exit from the growth region, probably because they drop out from the carrier gas stream, owing to their high gravity. On the contrary, a large number of small clusters are observed there. These results indicate that the nucleation and growth occur in a wide range at high P_{Ar} and V_{Ar}.

4 Discussion

Precise control of the nucleation and growth processes is a key point for monodispersive cluster formation. However, it is difficult to control these processes in the conventional gas evaporation method, because the clusters nucleate and grow rapidly in a narrow region just above an evaporation source [6, 7]. When we use a carrier gas flow system, we can

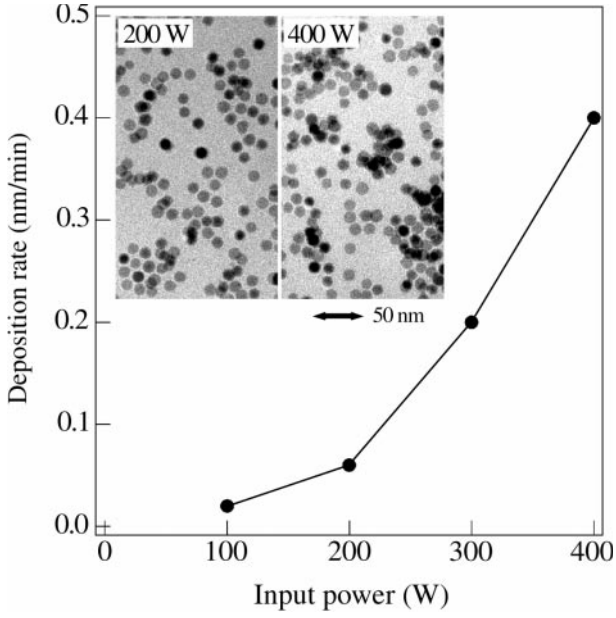

Fig. 4. Typical deposition rate as a function of the sputter power at the Ar gas pressure, $P_{\mathrm{Ar}} = 170\,\mathrm{Pa}$. In the inset of the figure are bright–field TEM images of Cr clusters produced at 200 and 400 W.

extend the nucleation and growth regions [8]. Indeed, the nucleation does not occur near the sputtering source at low P_{Ar} in the present experiments, as can be seen in Fig. 5. Hence, we can control the nucleation and growth processes independently in the present PGC apparatus.

As shown in Fig. 5, moreover, the nucleation and growth are restricted only in the liquid nitrogen-cooled growth region under the monodispersive cluster formation condition ($P_{\mathrm{Ar}} = 170\,\mathrm{Pa}$, i.e., $V_{\mathrm{Ar}} = 5.0 \times 10^{-6}\,\mathrm{m}^3/\mathrm{s}$), while it extends over a wide region under the broad-sized cluster formation condition ($P_{\mathrm{Ar}} = 280\,\mathrm{Pa}$, i.e., $V_{\mathrm{Ar}} = 1.0 \times 10^{-5}\,\mathrm{m}^3/\mathrm{s}$). We can understand the above results in terms of the nucleation theory [9]. At low P_{Ar} (170 Pa), the sputtered metal vapor is carried into the growth region without nucleation, and then cooled effectively by liquid nitrogen. This leads to a rapid increase in the supersaturation ratio of the sputtered metal vapor, promoting the nucleation process. Since the sputtered metal atoms are rapidly consumed by atom absorption during the nucleation, the supersaturation ratio decreases rapidly. This results in a short nucleation period. After the nucleation process finished, only the stable nuclei exceeding a critical size grow without further nucleation. Such instantaneous nucleation and subsequent growth of nuclei clearly separate the nucleation and growth stages, leading to the monodispersive cluster formation. At high P_{Ar} (280 Pa), on the other hand, clusters nucleate and grow even near the sputtering source, where the formed clusters grow by both atom absorption and coagulation, because the density in the number of sputtered metal atoms near the target is larger than that in the growth region. Moreover, the cluster formation process extends over the wide region from the sputtering source to the entire growth region. Hence, the

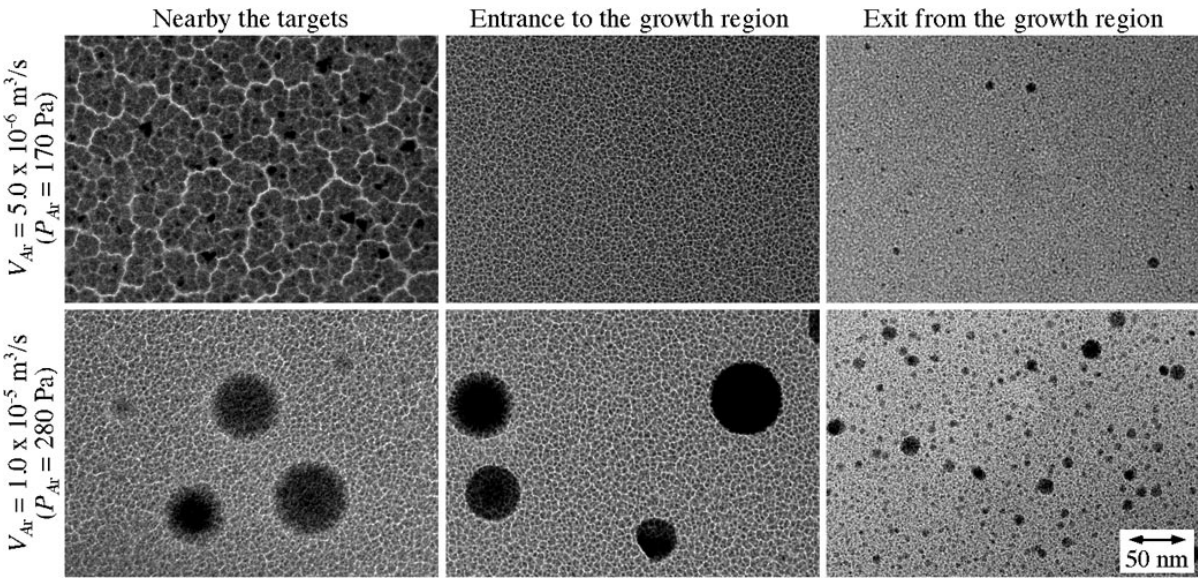

Fig. 5. Bright-field TEM images of Cr clusters deposited at different Ar gas pressures, P_{Ar}, of 170 and 280 Pa, and at different positions. The samples were deposited near the sputtering target, at the entrance to the growth region, and at the exit from the growth region. The Ar gas flow rate, V_{Ar}, was also varied with P_{Ar}.

nucleation and growth stages are not separated clearly, and the size distribution becomes broad.

In our previous works [3, 4], we reported that the deposition rate was rather low when we obtained the monodispersive clusters at low P_{Ar}, while it becomes higher when we obtained the broad-sized clusters at high P_{Ar}. In addition, the number of clusters deposited at the exit from the growth region at low P_{Ar} is lower than that at high P_{Ar}, as is shown in Fig. 5. These results indicate that the number density of nuclei is low under the monodispersive cluster formation condition, while it is high under the broad-sized cluster formation condition. Therefore, the collisions among clusters or nuclei hardly occur at low P_{Ar}, preventing the coagulation of the clusters; while they will easily occur at high P_{Ar}. Consequently, it is important to separate the nucleation and growth stages distinctly and to prohibit the coagulation of the growing particles if monodispersive clusters are to be produced. These conditions are similar to those of monodispersive colloidal particle formation [10].

The large amount of carrier gas also broadens the dispersion of the cluster size distribution, as is shown in Figs. 2 and 3. At this moment, the effect of carrier gas flow on the size distribution is not well understood. However, it is probably attributable to turbulent flow generation near the targets at high V_{Ar}, because the gas inlet having a small internal diameter (4 mm) generates a fast gas flow whose Reynolds number (e.g., ~ 4000 at $V_{Ar} = 1.42 \times 10^{-6}\,m^3/s$) is large enough for the turbulence. For a detailed understanding, it is necessary to perform a computer simulation of the gas stream, including metal clusters in the sputtering chamber and the growth region. Moreover, the low-temperature process of the sputtering technique will be also favorable for producing monodispersive clusters, because it suppresses the coalescence growth.

5 Conclusion

We have deposited nanometer-sized Cr clusters on TEM microgrids by the plasma-gas-condensation (PGC) method, and observed them by TEM. The monodispersive Cr clusters were obtained in the size rage of 8.5–13 nm at low Ar gas pressure, P_{Ar}, and low Ar gas flow rate, V_{Ar}. At low P_{Ar}, the nucleation and growth occur only in the liquid nitrogen-cooled growth region, and the deposition rate is rather low. At high P_{Ar}, on the other hand, a number of large clusters are formed even near the sputtering source, and the nucleation and growth regions extend from the sputtering source to the growth region. Under this condition, the deposition rate is relatively high. These results demonstrate that the nucleation and growth processes are definitely separated and that the coagulation of growing clusters is prohibited. In the present experiments, these conditions are achieved effectively by use of the carrier gas flow and liquid nitrogen cooling of the cluster growth process.

This work was supported by Core Research for Evolutional Science and Technology (CREST) of Japan Science and Technology Corporation (JST). We are also indebted to the Laboratory for Developmental Research of Advanced Materials in our Institute (IMR) for its support.

References

1. P. Melinon, V. Paillard, V. Dupuis, A. Perez, P. Jensen, A. Hoareau, J.P. Perez, J. Tuaillon, M. Broyer, J.L. Vialle, M. Pellarin, B. Baguenard, J. Lerme: Int. J. Mod. Phys. B **9**, 339 (1995)

2. S. Yamamuro, M. Sakurai, K. Sumiyama, K. Suzuki: AIP Conf. Proc. **416**, 491 (1998)
3. S. Yamamuro, M. Sakurai, K. Sumiyama, K. Suzuki: Supramol. Sci. **5**, 239 (1998)
4. S. Yamamuro, K. Sumiyama, K. Suzuki: J. Appl. Phys. **85**, 483 (1999)
5. H. Haberland, M. Karrais, M. Mall, Y. Thurner: J. Vac. Sci. Technol. A **10**, 3266 (1992)
6. S. Yatsuya, S. Kasukabe, R. Uyeda: Jpn. J. Appl. Phys. **12**, 1675 (1973)
7. C.G. Granqvist, R.A. Buhrman: J. Appl. Phys. **47**, 2200 (1976)
8. S. Iwama, K. Hayakawa: Nanostruct. Mater. **1**, 113 (1992)
9. V.K. LaMer, R.H. Dineger: J. Am. Chem. Soc. **72**, 4847 (1950)
10. T. Sugimoto: Adv. Colloid Interface Sci. **28**, 65 (1987)